HOSTED BY

ELSEVIER

Available online at www.sciencedirect.com

ScienceDirect

Journal of Sport and Health Science 6 (2017) 489–497

www.jshs.org.cn

Original article

Three-dimensional impact kinetics with foot-strike manipulations during running

Andrew D. Nordin *, Janet S. Dufek, John A. Mercer

Department of Kinesiology and Nutrition Sciences, University of Nevada, Las Vegas, NV 89154, USA

Received 15 March 2015; revised 18 June 2015; accepted 2 September 2015

Available online 11 November 2015

Abstract

Background: Lack of an observable vertical impact peak in fore/mid-foot running has been suggested as a means of reducing lower extremity impact forces, although it is unclear if impact characteristics exist in other axes. The purpose of the investigation was to compare three-dimensional (3D) impact kinetics among foot-strike conditions in over-ground running using instantaneous loading rate–time profiles.

Methods: Impact characteristics were assessed by identifying peak loading rates in each direction (medial–lateral (ML), anterior–posterior (AP), vertical, and 3D resultant) following foot-strike instructions (fore-foot, mid-foot, subtle heel, and obvious heel strike). Kinematic and kinetic data were analyzed among 9 male participants in each foot-strike condition.

Results: Loading rate peaks were observed in each direction and foot-strike condition, differing in magnitude by direction (3D resultant and vertical > AP > ML, $p \le 0.031$) and foot-strike: ML (fore-foot and mid-foot strike > obvious heel strike, $p \le 0.032$), AP (fore-foot and mid-foot strikes > subtle-heel and obvious heel strikes, $p \le 0.023$). In each direction, the first loading rate peak occurred later during heel strike running relative to fore-foot ($p \le 0.019$), with vertical and 3D resultant impact durations exceeding shear (ML and AP, $p \le 0.007$) in each condition.

Conclusion: Loading rate–time assessment identified contrasting impact characteristics in each direction and the 3D resultant following foot-strike manipulations, with potential implications for lower extremity structures in running.

Keywords: Fore-foot; Heel strike; Loading rate; Mid-foot; Overground; Resultant

1. Introduction

Interactions among running mechanics, impact kinetics, and overuse injuries represent a significant area of biomechanics research. Foot-strike patterns (i.e., the manner in which the foot contacts the ground during running) can influence impact characteristics as measured by the ground reaction force (GRF) versus time plot (GRF–time).[1] Hypotheses relating impact forces and overuse injuries have specifically been concentrated on the high-frequency impact peak in the vertical ground reaction force,[1–9] occurring during the first 50 ms after the foot collides with the ground.[10] Lack of an observable vertical impact peak in the GRF–time series during fore/mid-foot running has been suggested as a possible means of reducing impact loads on lower extremity tissues.[6] Exclusive analysis of the vertical direction, however, may overlook impact characteristics in other axes, particularly following subtle alterations within the spectrum of available foot-strike patterns.[2] Collectively, complete understanding of the interactions among running mechanics, patterns of force application, and injury rates has yet to be reached.[3,4,6,7,9,11–14] Examining three-dimensional (3D) changes in impact kinetics during foot-strike manipulations may therefore shed additional light into altered loading patterns in running.

Previous research has highlighted 3D changes in impact kinetics during fore-foot running, relative to rear-foot running, with impact peaks documented in the anterior–posterior (AP) and medial–lateral (ML) GRFs.[1,2,7] Although measurement of 3D kinetics is common, examining impact characteristics in each axis independently and in combination via the 3D resultant may provide more comprehensive insight into the magnitude and direction of applied forces.[2] High-frequency shear forces applied to the structures of the fore- and mid-foot,

Peer review under responsibility of Shanghai University of Sport.

* Corresponding author.

E-mail addresses: nordina@unlv.nevada.edu; nordina@umich.edu (A.D. Nordin).

Current address: School of Kinesiology, University of Michigan, Ann Arbor, MI 48109, USA.

https://doi.org/10.1016/j.jshs.2015.11.003

including the metatarsal heads, plantar fascia, and toe flexor muscles, may highlight contrasting mechanisms of injury in each respective foot-strike pattern relative to rear-foot strike.[2,11,15] Thus, the location, direction, magnitude, and patterns of force application are each considered important in understanding the implications of foot-strike manipulations, potentially relocating the site of injury rather than mitigating the cause.

Extending beyond examinations of GRF magnitudes, loading rate characteristics have been used in exploring injury mechanisms in running.[2,4,6,12,13] Instantaneous and average vertical loading rates have each been examined during initial ground contact, with lesser and equivalent vertical loading rates reported in fore- versus rear-foot shod running.[2,4,6,12,13] Despite equivocal vertical loading rate findings following foot-strike manipulations, instantaneous 3D loading rate–time patterns may provide additional means of identifying changes in impact kinetics.[2] Boyer et al.[2] previously demonstrated contrasting instantaneous 3D loading rate magnitudes following foot-strike pattern manipulations in competitive runners exhibiting different habitual foot-strike patterns. Assessing loading rate–time characteristics across a wider range of foot-strike patterns is therefore considered beneficial, with attention directed toward magnitude and temporal features of the 3D loading rate–time series.

Differentiation of the GRF–time curve amplifies higher frequency components, potentially making the loading rate–time curve more sensitive in detecting impact characteristics, while maintaining the temporal features of the signal.[16] Assessment of the loading rate–time curve may therefore allow identification of subtle impact characteristics in the GRF–time curve in foot-strike conditions that appear to lack GRF impact peaks; the typical case in vertical GRF during fore/mid-foot running.[1–3,5] It is, however, acknowledged that the GRF represents the summation of force components from the total body and may therefore contain features not directly related to impact, or to the lower extremity.[10,16,17] Nevertheless, the challenge of comparing impact characteristics among foot-strike conditions is the lack of observable force peaks in particular axes and foot-strike patterns (e.g., vertical GRF during fore/mid-foot strike running). All GRF–time profiles can, however, be assessed using loading rate characteristics. Particular attention can be directed toward initial loading, during braking (prior to the zero crossing of the anterior–posterior GRF and the overall vertical GRF peak), where short duration fluctuations in the GRF and loading rate–time curves can be attributed to impact characteristics during foot–ground collision. Characterizing the impact phase using the loading rate–time profile may therefore be useful in examining interactions among foot-strike patterns and impact kinetics.

The purpose of the investigation was to compare 3D impact kinetics among foot-strike conditions in over-ground running using instantaneous loading rate–time profiles. Impact characteristics were operationally defined using loading rate peak magnitudes and temporal features for each direction (ML, AP, vertical, and 3D resultant) following specific foot-strike instructions (fore-foot strike, mid-foot strike, subtle heel strike, obvious heel strike). Descriptive GRF impact magnitudes were also examined.

It was hypothesized that impact forces always exist in running; therefore, 3D assessment of the instantaneous loading rate–time profile would allow subtle impact characteristics to be identified from the GRF. Furthermore, it was hypothesized that loading rate characteristics (temporal and magnitude) would differ by direction and foot-strike condition, with peak loading rate occurring sooner in the ML and AP directions during fore- and mid-foot striking, but with greater magnitude and duration in the vertical direction during heel striking.

2. Materials and methods

2.1. Participants

Nine male recreational runners (age 26.0 ± 4.7 years, height 1.75 ± 0.03 m, mass 79.8 ± 7.4 kg; mean ± SD), free from lower extremity injury and physically active at least 2 days per week, volunteered to participate in the study. Written informed consent was obtained for each participant prior to participation as approved by the Las Vegas Office of Research Integrity-Human Subjects of University of Nevada, in compliance with the Declaration of Helsinki. Participants each wore standardized neutral running shoes of appropriate size (response competition; Adidas, Herzogenaurach, Germany). Of the 9 participants, 5 self-identified as natural fore/mid-foot strike runners, with 4 identified as heel-strike runners; self-identification and visual experimenter examination were carried out during treadmill warm-up.

2.2. Procedures

A treadmill warm-up was completed, simultaneously obtaining preferred running speed suitable for a 30 min jog. Participants were blinded to treadmill controls, and belt speed was adjusted until a desired running speed was selected (3.3 ± 0.4 m/s). Approximately 5 min accommodation periods were provided for each participant.

Over-ground running trials were performed along a 20 m runway, providing practice trials to ensure each participant was comfortable contacting a force platform embedded in the ground with the right foot, without targeting. Foot-strike conditions included fore-foot strike, mid-foot strike, subtle heel strike, and obvious heel strike. Periods of rest from 30 s to 1 min were provided between each trial, with several minutes provided between conditions in an attempt to reduce participant fatigue. Participants were provided instructional videos illustrating the desired foot-strike patterns, with participants verbally instructed to match the demonstrated foot-strike pattern to the best of their ability. Practice trials were provided (typically 1–5 trials), allowing participants to perform each foot-strike condition prior to collected trials. Participants ran through timing gates synchronized via a multi-function timer, separated by 7 m (Model 63501IR and 54035A, respectively; Lafayette Instrument, Lafayette, IN, USA). Trials outside of an acceptable time window (±5% preferred speed) were discarded and repeated, along with trials visibly altered in an attempt to contact the force platform or deviating from the desired foot-strike pattern. Participants were considered acclimated once the desired foot-strike pattern, target running speed, and foot

placement were visibly established in each condition. Blocked foot-strike conditions were carried out in randomized order for each participant. Participants completed 15 successful trials (10 trials used during analysis) in 4 foot-strike conditions (60 trials total, 4 conditions × 15 trials per condition).

2.3. Data analysis

Kinetic data were acquired using a force platform (9281CA; Kistler, Winterhur, Switzerland; 2000 Hz), with synchronized sagittal plane reference video of the foot contacting the force platform for visual corroboration of each foot-strike pattern (piA640-210gc; Basler, Ahrensburg, Germany; CCTV lens C60812; Pentax, Tokyo, Japan; sample rate: 50 Hz, shutter speed: 6 ms). Trials deviating from the desired foot-strike pattern during visual assessment of foot-strike pattern from sagittal reference video were excluded from analysis; otherwise, the last 10 trials in each condition were used during analysis. Kinetic data were low-pass filtered with a cutoff of 50 Hz using a 4th order (0 lag) Butterworth filter, determined through visual inspection of fast Fourier transform harmonics and power spectral density (MATLAB R2012a; Mathworks, Natick, MA, USA). Kinematic data were collected using a 12-camera motion capture system and 35-point spatial model (Plugin Gait Full Body; Vicon, Oxford, UK; 200 Hz), with marker trajectories low-pass filtered (Butterworth 4th order) at a cutoff frequency of 15 Hz. Foot segment angle at contact, relative to the ground, was used for additional verification of foot-strike pattern.[18] Data were analyzed across the stance phase of running for the right limb.

Data reduction was carried out via custom M scripts (R2012a), identifying vertical, AP, ML, and 3D resultant GRF–time profiles with forces in each direction normalized to body weight (BW). The stance phase of each trial was identified from the point of ground contact (vertical GRF > 20 N) to the point of takeoff (vertical GRF < 20 N). For consistent expression of positive GRF and loading peaks, positive GRF values indicate superior, posterior, and medial directions, respectively. Special consideration was given for the ML direction due to the presence of lateral impact characteristics. Statistical analysis was performed using the aggregated absolute value of the medial and lateral loading peaks. Due to the possibility of multiple GRF peaks occurring within an axis during impact, or the absence of an observable GRF peak, the aim was to identify the primary impact phase in each direction using instantaneous loading time computed via first central difference differentiation.

For the purpose of this study, an impact peak was defined as occurring when a maximum force peak preceded a minimum force peak during braking (Fig. 1). Fig. 1 illustrates a typical

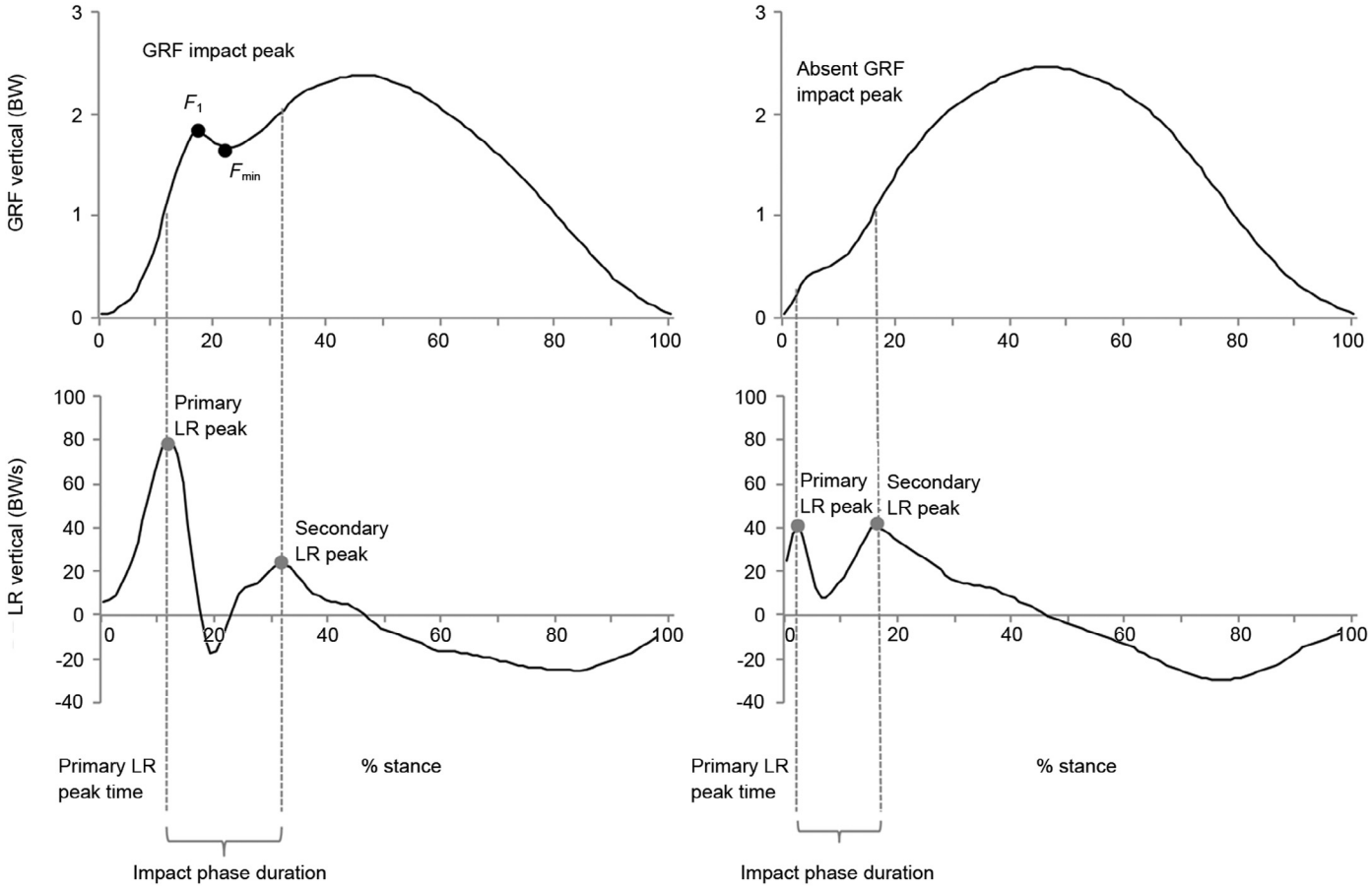

Fig. 1. Exemplar identification of impact phase from loading rate (LR) and ground reaction force (GRF) peaks. BW = body weight; F_1 = impact peak; F_{min} = local minimum force.

GRF–time series that includes a GRF impact peak (F_1) followed by a local minimum force (F_{min}). When an impact peak was present, a maximum loading rate peak would precede the GRF impact peak (F_1), followed by a loading rate minimum (loading rate < 0; Fig. 1). Similarly, a loading rate minimum would precede the GRF minimum (F_{min}) followed by a maximum loading rate peak (Fig. 1). Since it was expected that an observable GRF peak would not be present in some conditions, the loading rate–time curve was used to identify impact peak regions for each direction. If multiple impact regions existed within an axis, the portion of the loading rate–time curve with the greatest cumulative magnitude change between successive instantaneous loading rate maxima was used in identifying the primary impact phase (Fig. 1).

The first local loading maximum was identified as the primary loading rate peak, with the next local loading maximum identified as the secondary loading rate peak (Fig. 1). Instantaneous loading rate–time characteristics were therefore used in delimiting the impact phase (portion of stance from the primary to secondary loading rate peak), defining magnitude and temporal features of impact, and identifying the primary GRF impact peak within a trial, when present.

Dependent variables included primary loading rate peak magnitude (BW/s), time of primary loading rate peak occurrence (second), and impact duration (operationally defined as time from primary to secondary loading rate peak; second) in each direction (ML, AP, vertical, and 3D resultant; Fig. 1). Additionally, GRF impact magnitude (F_1; BW) was examined descriptively (Fig. 1).

2.4. Statistical analysis

Statistical analysis was carried out using primary loading rate peak magnitude, time of primary loading rate peak occurrence, and impact duration via separate 4 × 4 (foot-strike (fore-foot, mid-foot, subtle-heel, obvious heel strike)) × (direction (ML, AP, vertical, 3D resultant)) repeated measures ANOVAs (SPSS Statistics Version 23.0; IBM Corp., Armonk, NY, USA). If there was a significant interaction for any dependent variables, simple main effects analysis was performed via one-way repeated measures ANOVAs for each factor, with pairwise comparisons identifying the location of significant differences. Effect size was expressed using partial η^2 (small: $\eta^2 = 0.01$, medium: $\eta^2 = 0.06$, large: $\eta^2 = 0.14$).[19] Degrees of freedom were adjusted via Huynh–Feldt corrections as necessary.[19] Alpha level for *post hoc* contrasts was adjusted via Sidak corrections ($\alpha = 0.05$). A one-way repeated measures ANOVA was used in comparing foot segment angle at contact among foot-strike conditions ($\alpha = 0.05$).

3. Results

3.1. Descriptive characteristics

Loading rate peaks were observed in the loading rate–time curves during initial ground contact in each direction and foot-strike condition (Figs. 2 and 3A). Ensemble GRF and loading rate–time curves are presented for each direction (ML, AP, vertical, and 3D resultant) and foot-strike condition (Fig. 2). Primary loading rate peak magnitudes are summarized by direction and foot-strike condition (Fig. 3A). GRF impact peak magnitudes and the number of trials with observable impact peaks are summarized by foot-strike condition and direction (Table 1). Foot segment angle at contact differed among foot-strike conditions, supporting the distinction among foot-strike patterns (fore-foot strike: −12.0° ± 4.5°; mid-foot strike: −0.9° ± 8.8°; subtle-heel strike: 10.9° ± 7.4°; obvious heel strike: 16.9° ± 4.7°; $F(3, 24) = 37.9$, $p < 0.001$, $\eta^2 = 0.27$; pairwise comparisons: $p \leq 0.013$).[18]

Lateral primary loading rate peaks were aggregated with medial primary loading rate peaks in the ML direction, but had similar magnitude (BW/s) and temporal (time of occurrence; second) characteristics (lateral primary loading rate peak: 27 mid-foot strike trials (13.6 ± 5.9 BW/s, 0.017 ± 0.009 s), 25 subtle heel strike trials (8.8 ± 5.2 BW/s, 0.022 ± 0.004 s), and 31 obvious heel strike trials (7.7 ± 4.4 BW/s, 0.025 ± 0.013 s). Similarly, trials with lateral GRF impact peaks were combined with medial peaks in the ML summary (lateral GRF peaks: 10 mid-foot strike trials (0.04 ± 0.03 BW), 7 subtle-heel strike trials (0.03 ± 0.03 BW), and 3 obvious heel strike trials (0.02 ± 0.02 BW)). GRF impact peaks were observed in each direction and foot-strike condition, but with contrasting magnitude and number of occurrence (Table 1).

3.2. Impact magnitude

Primary loading rate peak magnitude differences were observed among axes and foot-strike conditions (Fig. 3A). Primary loading rate peak magnitude was influenced by the interaction of foot-strike and direction ($F(9, 72) = 3.0$, $p = 0.004$, $\eta^2 = 0.27$). In each foot-strike condition, primary loading rate peaks in the vertical direction and 3D resultant exceeded those in the ML and AP directions ($p \leq 0.002$), with those in the AP direction further exceeding the ML direction ($p \leq 0.031$). In the fore-foot strike condition, primary loading rate peaks in the 3D resultant exceeded primary loading rate peaks in the vertical direction ($p = 0.007$). With respect to foot-strike differences, AP primary loading rate peaks during fore- and mid-foot strike conditions exceeded those in subtle heel and obvious heel strike conditions ($p \leq 0.023$), while ML primary loading rate peaks during fore- and mid-foot strike conditions exceeded those in the obvious heel strike condition ($p \leq 0.032$). Overall, magnitude differences were observed among axes in each foot-strike condition (R and Z > Y > X), with additional differences observed among foot-strike conditions in the ML (fore- and mid-foot > obvious heel strike) and AP directions (fore- and mid-foot > subtle and obvious heel strike).

3.3. Impact onset

Time of primary loading rate peak occurrence differed among foot-strike conditions (Fig. 3B). It was not influenced by the interaction of foot-strike and direction ($F(9, 72) = 0.6$, $p = 0.829$, $\eta^2 = 0.07$). The main effect for foot-strike was significant ($F(1.7, 14.0) = 8.7$, $p = 0.004$, $\eta^2 = 0.52$), while the main effect for direction was not statistically significant ($F(1.2,$

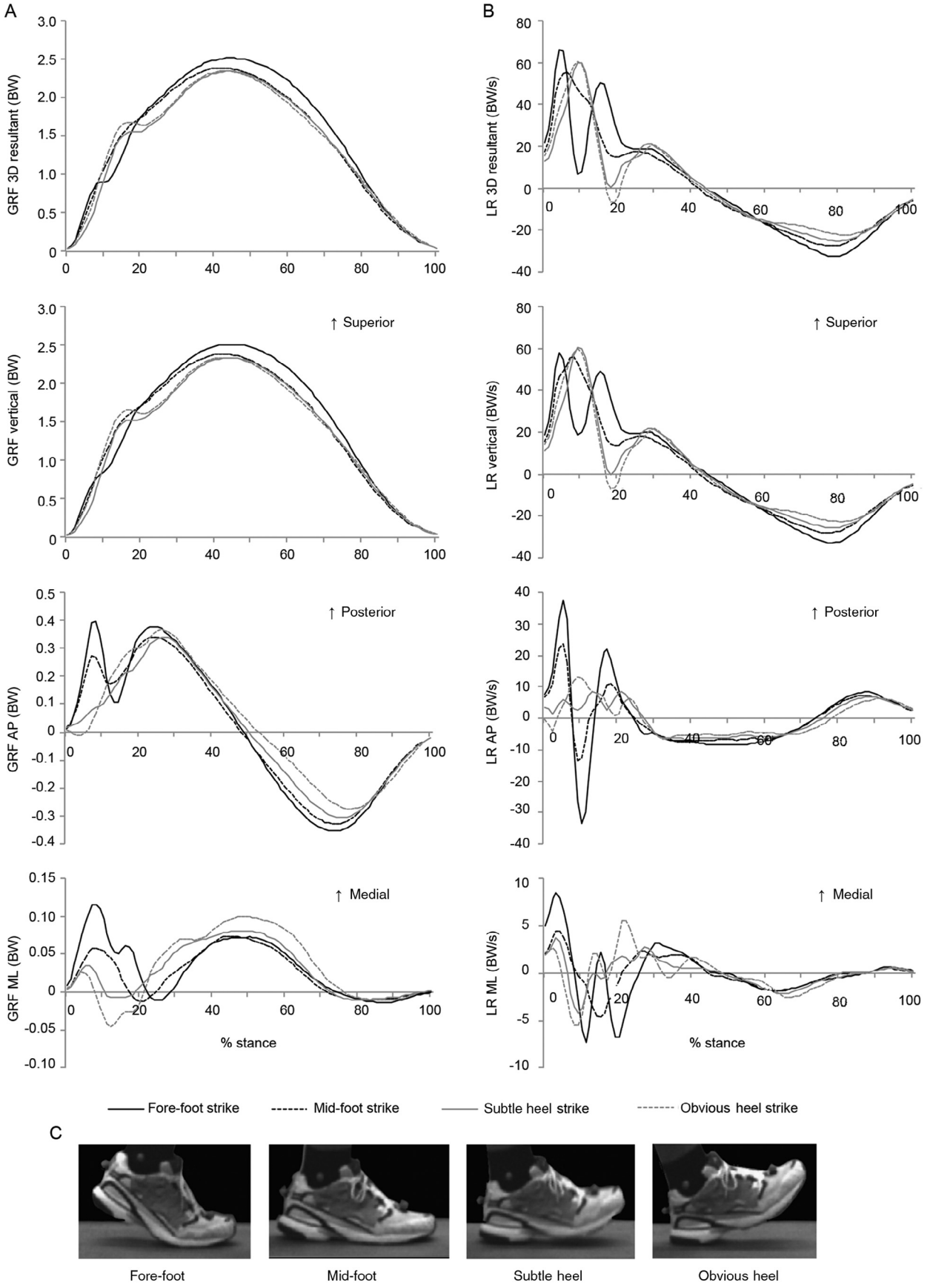

Fig. 2. Ensemble GRF (A) and loading rate (B) versus time curves by direction (3D resultant, vertical, AP, ML) and foot-strike (C). 3D = three dimensional; AP = anterior–posterior; BW = body weight; GRF = ground reaction force; LR = loading rate; ML = medial–lateral.

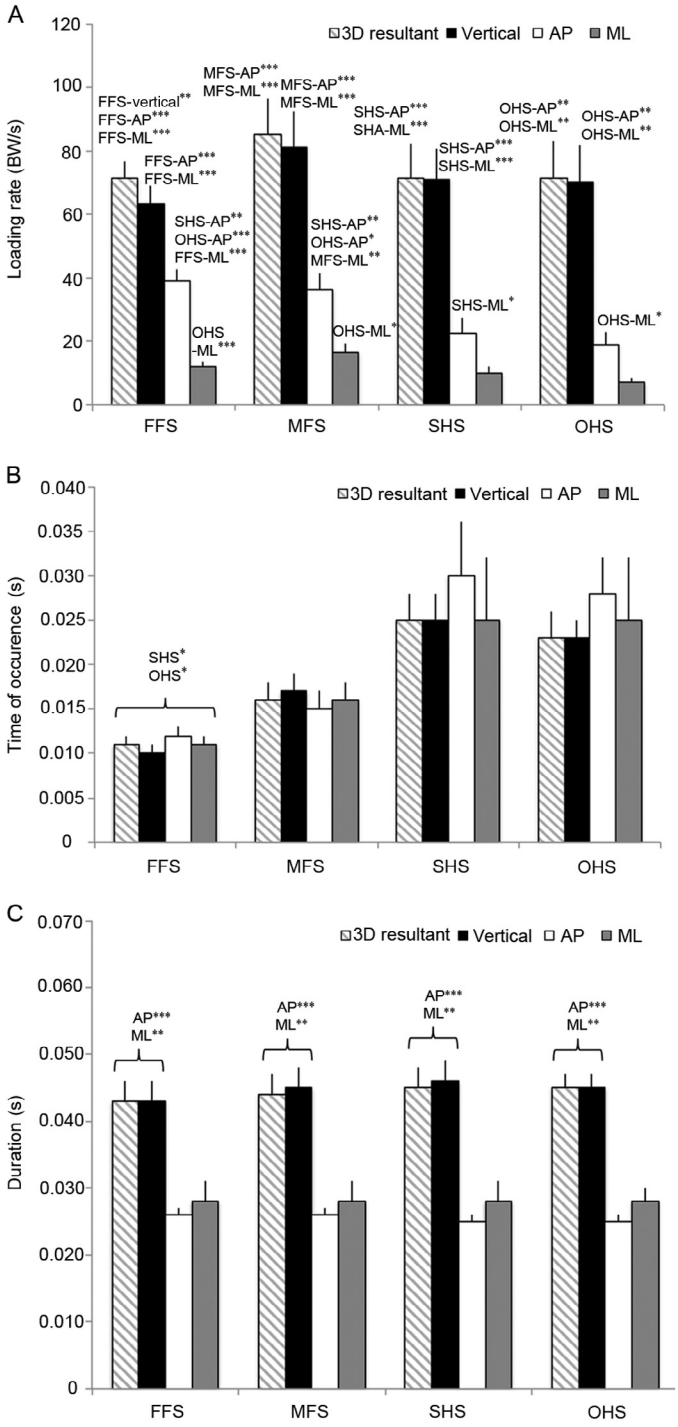

Fig. 3. Mean ± SE primary loading rate peak magnitude (A), loading rate peak time of occurrence (B), and impact duration (C; time from primary to secondary loading rate peak) by direction (3D resultant, vertical, AP, ML) and foot-strike. Significant differences highlighted by foot-strike and direction (A), foot-strike (B), and direction (C) (Sidak *post hoc* contrasts, $p < 0.05$). *$p < 0.05$, **$p \leq 0.01$, ***$p \leq 0.001$. AP = anterior–posterior; FFS = fore-foot strike; MFS = mid-foot strike; ML = medial–lateral; OHS = obvious heel strike; SHS = subtle heel strike.

9.8) = 0.6, $p = 0.507$, $\eta^2 = 0.07$). In each direction, primary loading rate peak occurred significantly later during subtle heel and obvious heel strike conditions relative to the fore-foot strike condition.

3.4. Impact duration

Impact duration differed among directions (Fig. 3C). It was not influenced by the interaction of foot-strike and direction ($F(9, 72) = 1.3$, $p = 0.269$, $\eta^2 = 0.14$). The main effect for direction was significant ($F(1.5, 11.8) = 26.8$, $p < 0.001$, $\eta^2 = 0.77$), while the main effect for foot-strike was not statistically significant ($F(1.2, 9.9) = 0.8$, $p = 0.434$, $\eta^2 = 0.09$). In each foot-strike condition, the impact duration in the 3D resultant and vertical direction significantly exceeded the ML and AP impact durations.

4. Discussion

In support of the outlined hypotheses, impact characteristics were observed in each direction and the 3D resultant during each foot-strike condition using the instantaneous time profile (Table 1). Earlier onset of short duration shear forces may highlight lower extremity injury mechanisms following foot-strike manipulations, with particular consideration for greater magnitude shear loads in fore/mid-foot running relative to heel-strike running.

4.1. Analysis considerations

Limitations are recognized in this investigation, including the experimentally controlled setting, the use of standardized shoes that may have been unfamiliar to participants, and the controlled running speed, which may naturally differ among foot-strike patterns. As well, given the cross-sectional nature of the investigation, the longitudinal effects of the observed kinetic characteristics are unknown. Further considerations include the familiarity of each participant with the instructed foot-strike patterns. Although instructional videos were provided, as well as practice trials, impact characteristics may differ with movement pattern accommodation.[2] The relatively small sample size and heterogeneity in habitual foot-strike patterns in the sampled participants may also limit generalizations to specific subsets of runners.

Beyond considerations for the study design, limitations are acknowledged in the measurement tools used in this investigation, including the methods of foot-strike pattern identification and the use of force platform analysis in the context of factors related to lower extremity injury. Foot-strike patterns were identified using foot segment angle at contact, providing insight into the position of the toe relative to the heel, which is sensitive to marker placement and reliant on a simplified foot segment model. For these reasons, sagittal video of the foot during ground contact was used in corroborating foot-strike patterns, providing an additional means of trial exclusion (10 trials used during analysis, 15 collected in each condition). Foot-strike pattern misclassifications were possible, however, due to marker placement errors and the relatively low sagittal reference video sampling rate. Although foot segment angles demonstrated statistical differences among conditions, future work may benefit from continuous foot-strike pattern classifications, rather than using discrete categories. With respect to the variables analyzed in this study, caution must be exercised regarding interpretations surrounding causative mechanisms and links

Table 1
Impact peak magnitude body weight.

Foot-strike	3D resultant			Vertical			Anterior–posterior			Medial–lateral		
	n	*M*	*SD*	*n*	*M*	*SD*	*n*	*M*	*SD*	*n*	*M*	*SD*
Fore-foot	48	0.92	0.30	22	0.71	0.41	90	0.41	0.11	86	0.14	0.05
Mid-foot	49	1.42	0.63	34	1.67	0.54	87	0.38	0.13	84	0.13	0.10
Subtle heel	61	1.58	0.49	62	1.56	0.47	73	0.27	0.14	87	0.07	0.08
Obvious heel	74	1.81	0.58	75	1.77	0.57	42	0.37	0.18	77	0.06	0.04

Note: *n* is the number of trials with impact peak (*n* = 90 trials per condition).

to injury. Shorten and Mientjes[16] outlined a decoupling between the time of GRF impact peak occurrence and the peak pressure at the foot, proportional to impact attenuation, including footwear properties, as the GRF expresses the total body acceleration and not simply that of the lower extremity.[10,16,17] Nonetheless, the GRF is applied at the location of contact with the force platform, which varies with foot-strike pattern. For these reasons, interpretations of magnitude and temporal features of impact loading are considered useful in the context of the site and direction of force application.

Despite the limitations outlined by Shorten and Mientjes[16] with respect to inferences regarding shoe cushioning and GRF impact characteristics, shoe construction properties must be considered when interpreting the results from this investigation. Participants wore standard cushioned running shoes, with greater heel cushioning compared to the fore/mid-foot. Although the work of Shorten and Mientjes[16] was performed across footwear conditions of contrasting cushioning properties during heel strike running, peak vertical loading rate and mean power frequency (>10 Hz) were greater in lesser cushioned shoes, with earlier impact peak occurrence. During fore-foot strike running, earlier time of primary loading rate peak occurrence (Fig. 3B), greater AP and ML loading, relative to heel strike running (Fig. 3A), may be partially attributed to lesser cushioning in the fore-foot region of the shoe. Similar trends were observed during mid-foot strike running (Fig. 3A and B).

Impact duration, differing by direction (3D resultant and vertical > AP and ML; Fig. 3C) in each foot-strike condition, may highlight additional limitations of force platform analysis. Contributions of body weight to the vertical direction lead to magnitude discrepancies between axes (GRF: vertical > AP > ML), which present longer duration impact characteristics in the vertical direction and 3D resultant. Interpretations of magnitude and temporal characteristics of the 3D GRF, including loading rate, are logically representative of total body accelerations superimposed in each axis, and in combination via the 3D resultant. Contrasting interpretations may therefore be reached when examining each axis independently or in combination. Additionally, the secondary loading rate peak occurs later, with causative mechanisms that likely differ by foot-strike pattern. Despite the outlined limitations, defining the impact duration using primary and secondary loading rate peaks provides an objective means of delimiting the impact phase during braking that may be overlooked when assessing the GRF–time series over a pre-determined absolute time (e.g., 50 ms), while also preserving the temporal features of the signal. Subsequently, the location, direction, magnitude, and pattern of force application are considered essential in understanding the implications of the applied loads.

4.2. Impact magnitude and onset

Comparing the present results with those from previous studies, primary loading rate peak magnitudes (Fig. 3A) showed similarity when accounting for running speed.[2,4,6,9] In agreement with Laughton et al.,[4] primary loading rate peak differences were not detected between fore-foot and heel strike conditions in the vertical direction, with lesser AP primary loading rate peak values observed during heel strike conditions relative to the fore-foot strike condition (Fig. 3A). Other examinations, however, have demonstrated reduced vertical loading rate during fore-foot relative to heel strike running,[12,13] while only Boyer et al.[2] presented primary loading rate peak data for each axis and the 3D resultant. Ensemble instantaneous loading rate–time plots presented by Boyer et al.[2] demonstrated similarities with respect to earlier primary loading rate peak occurrence during fore-foot strike relative to heel strike running in each direction and the 3D resultant (Figs. 2 and 3B). Additionally, the authors reported vertical and 3D resultant impact peaks during heel strike running, with an absolute time of occurrence approximately double that of the ML and AP directions during fore-foot strike running.[2]

4.3. Impact duration

In the present investigation, interpretation of impact duration was viewed in the context of the frequency of force application, as measured from the GRF–time curve, which maintains the temporal features of the signal. Understanding that lesser time between primary and secondary loading rate peaks indicates a higher frequency of force application, examination of impact duration provides additional insight beyond time of primary loading rate peak occurrence. Notably, in each foot-strike condition, shorter impact duration was observed in the shear GRF components (ML and AP; Fig. 3C). These results are in agreement with Boyer et al.,[2] defining the impact phase in the vertical direction and 3D resultant as twice that of the ML and AP directions (vertical/3D resultant: 0–20% stance, ML/AP: 0–10% stance, respectively). Interpreted alongside primary loading rate peak magnitude and time of occurrence (Fig. 3A and B), shorter duration shear forces were observed in each foot-strike condition, while greater magnitude shear loads were observed during

fore-foot strike running, when compared with subtle and obvious heel strike conditions (Fig. 3C). Similar trends were observed during mid-foot strike running (Fig. 3).

Although the current research assessed impact duration, insight may be gleaned from frequency domain comparisons. Gruber et al.[20] reported greater vertical GRF amplitudes at higher frequencies (13–39 Hz) during heel strike running relative to fore-foot strike running. Additional frequency analyses during foot-strike manipulations have been performed using accelerometry. Higher vertical tibial acceleration frequencies have been reported during heel strike running relative to fore-foot strike running,[14] with greater power spectral density at higher frequencies during heel strike running, and at longer stride lengths.[14,21] Importantly, tibial accelerations during fore-foot strike running are attenuated by the ankle joint, which is bypassed during heel strike running.[14] Additionally, much of the work examining tibial accelerations during running has been performed uniaxially in the vertical direction, although evidence suggests that 3D analyses are necessary; large magnitude peak tibial accelerations have been reported in the anterior–posterior direction in running.[22]

4.4. Descriptive characteristics

Overall, the results from this investigation demonstrate agreement with Boyer et al.,[2] examining 3D loading rate magnitudes in heel and fore-foot strike running among competitive runners. Although statistical analysis was not performed using the GRF impact peak magnitudes or time of occurrence in the present study, descriptive characteristics including magnitudes and number of trials showing impact peaks were reported (Table 1). In contrast to previous research, impact peaks were observed in each direction and the 3D resultant in each foot-strike condition.[2] Greater impact peak occurrence was, however, observed in the ML and AP directions during fore- and mid-foot strike conditions, and in the vertical direction and 3D resultant during subtle heel and obvious heel strike conditions (Table 1). Typically, impact peaks are not reported in the vertical GRF during fore-foot strike running or in the AP and ML directions during heel strike running.[2,3,5] As a result, Boyer et al.[2] reported GRF magnitudes at the mean time of impact peak occurrence in rear-foot running, during fore/mid-foot conditions. A contrasting approach was taken in the present investigation, which might explain discrepancies between the results from each study; GRF impact magnitudes were approximately 1.5 times greater among axes in the results from Boyer et al.[2] Magnitude differences in GRF peaks may be attributed to running speed differences, while the detection of impact characteristics in each direction and foot-strike condition may highlight kinetic differences with contrasting levels of experience in the sampled runners in each study: competitive versus recreational.[2] Detection of lower magnitude vertical GRF peaks during fore-foot strike running is likely related to the earlier time of primary loading rate peak occurrence (Table 1, Fig. 3B), with greater 3D resultant impact peak occurrence in fore-foot strike trials, relative to vertical, highlighting the expression of shear impact features in the 3D resultant (Table 1).

4.5. Implications

Collectively, earlier onset of shorter duration shear loads may have implications for the structures of the fore/mid-foot in fore-foot and mid-foot running, with greater magnitude shear loads when compared with subtle heel and obvious heel strike conditions. Lower extremity overuse injuries in running have been reported to include stress fractures of the tibia and metatarsal heads,[9,11] as well as soft tissue injuries, including the plantar fascia, and toe flexor muscles, which act to moderate bone loads. Repetitive sub-maximal loading of structures in the vertical and shear directions may therefore lead to the accumulation of trauma that outpaces bone remodeling, with lesser tolerance reported for shear loads.[2,9,11]

5. Conclusion

Using a loading rate–time approach, impact characteristics were observed in each direction and the 3D resultant for each foot-strike condition. This observation emphasizes the importance of considering multi-axis force components when altering the manner in which the foot collides with the ground. Although limitations are recognized in the interpretations of GRF and loading characteristics as representative of impact features, loading magnitudes, time of occurrence, impact duration, site of load application, and direction provide additional considerations for potential injury mechanisms following foot-strike manipulations.

Acknowledgments

The authors would like to thank Sergio Castro and Josh Bailey for their assistance in data collection. This research was partially funded by the Institutional Development Award Network of Biomedical Research Excellence through the National Institute of General Medical Sciences (8 20 GM103440-11).

Authors' contributions

ADN collected and analyzed the data, and drafted the manuscript; JSD guided the analysis and helped draft the manuscript; JAM conceived of the study and its design and helped draft the manuscript. All authors have read and approved the final version of the manuscript, and agree with the order of author presentation.

Competing interests

The authors declare that they have no competing interests.

References

1. Cavanagh PR, Lafortune MA. Ground reaction forces in distance running. *J Biomech* 1980;**13**:397–406.
2. Boyer ER, Rooney BD, Derrick TR. Rearfoot and midfoot or forefoot impacts in habitually shod runners. *Med Sci Sports Exerc* 2014;**46**:1384–91.
3. Daoud AI, Geissler GJ, Wang F, Saretsky J, Daoud YA, Lieberman DE. Foot strike and injury rates in endurance runners: a retrospective study. *Med Sci Sports Exerc* 2012;**44**:1325–34.

4. Laughton CA, McClay Davis I, Hamill J. Effect of strike pattern and orthotic intervention on tibial shock during running. *J Appl Biomech* 2003;**19**:153–68.
5. Lieberman DE, Venkadesan M, Werbel WA, Daoud AI, D'Andrea S, Davis IS, et al. Foot strike patterns and collision forces in habitually barefoot versus shod runners. *Nature* 2010;**463**:531–5.
6. Shih Y, Lin KL, Shiang TY. Is the foot striking pattern more important than barefoot or shod conditions in running? *Gait Posture* 2013;**38**:490–4.
7. Williams III DS, McClay IS, Manal KT. Lower extremity mechanics in runners with a converted forefoot strike pattern. *J Appl Biomech* 2000;**16**:210–8.
8. Willson JD, Bjorhus JS, Williams 3rd DSB, Butler RJ, Porcari JP, Kernozek TW. Short-term changes in running mechanics and foot strike pattern after introduction to minimalistic footwear. *PMR* 2014;**6**:34–43.
9. Zadpoor AA, Nikooyan AA. The relationship between lower-extremity stress fractures and the ground reaction force: a systematic review. *Clin Biomech (Bristol, Avon)* 2011;**26**:23–8.
10. Bobbert MF, Schamhardt HC, Niqq BM. Calculation of vertical ground reaction force estimates during running from positional data. *J Biomech* 1991;**24**:1095–105.
11. Ridge ST, Johnson AW, Mitchell UH, Hunter I, Robinson E, Rich BS, et al. Foot bone marrow edema after a 10-wk transition to minimalist running shoes. *Med Sci Sports Exerc* 2013;**45**:1363–8.
12. Cheung RT, Davis IS. Landing pattern modification to improve patellofemoral pain in runners: a case series. *J Orthop Sports Phys Ther* 2011;**41**:914–9.
13. Diebal AR, Gregory R, Alitz C, Gerber JP. Forefoot running improves pain and disability associated with chronic exertional compartment syndrome. *Am J Sports Med* 2012;**40**:1060–7.
14. Gruber AH, Boyer KA, Derrick TR, Hamill J. Impact shock frequency components and attenuation in rearfoot and forefoot running. *J Sport Health Sci* 2014;**3**:113–21.
15. Arangio GA, Beam H, Kowalczyk G, Salathe EP. Analysis of stress in the metatarsals. *Foot Ankle Surg* 1998;**4**:123–8.
16. Shorten M, Mientjes MIV. The "heel impact" force peak during running is neither "heel" nor "impact" and does not quantify shoe cushioning effects. *Footwear Sci* 2011;**3**:41–58.
17. Winter DA. *Biomechanics and motor control of human movement*. 4th ed. Hoboken, NJ: John Wiley & Sons, Inc.; 2009.
18. Altman AR, Davis IS. A kinematic method for footstrike pattern detection in barefoot and shod runners. *Gait Posture* 2012;**35**:298–300.
19. Field A. *Discovering statistics using SPSS*. 3rd ed. Thousand Oaks, CA: SAGE Publications Ltd.; 2009. p.461.
20. Gruber AH, Davis IS, Hamill J. Frequency content of the vertical ground reaction force component during rearfoot and forefoot running patterns. *Med Sci Sports Exerc* 2011;**43**:60. doi:10.1249/01.MSS.0000402852.25234.f0
21. Mercer JA, Devita P, Derrick TR, Bates BT. Individual effects of stride length and frequency on shock attenuation during running. *Med Sci Sports Exerc* 2003;**35**:307–13.
22. Lafortune MA. Three-dimensional acceleration of the tibia during walking and running. *J Biomech* 1991;**24**:877–86.